# Engineering g-$C_3N_4$ composited Fe-UIO-66 to in-situ generate robust single-atom Fe sites for high-performance PEMFC and Zn-air battery

Lu An[a,1], Bin Chi[a,1], Yingjie Deng[a], Chao Chen[a], Xiaohua Deng[a], Ranjie Zeng[a], Yuying Zheng[a], Dai Dang[a]*, Xu Yang [a]*, Xinlong Tian [b]*

[a] *School of Chemical Engineering and Light Industry, Guangdong University of Technology, Guangzhou, 510006, P. R. China*

[b] *State Key Laboratory of Marine Resource Utilization in South China Sea, Hainan Provincial Key Lab of Fine Chemistry, School of Chemical Engineering and Technology, Hainan University, Haikou 570228, China*

*Corresponding author E-mail address: dangdai@gdut.edu.cn

[1] Lu An and Bin Chi contributed equally to this work.

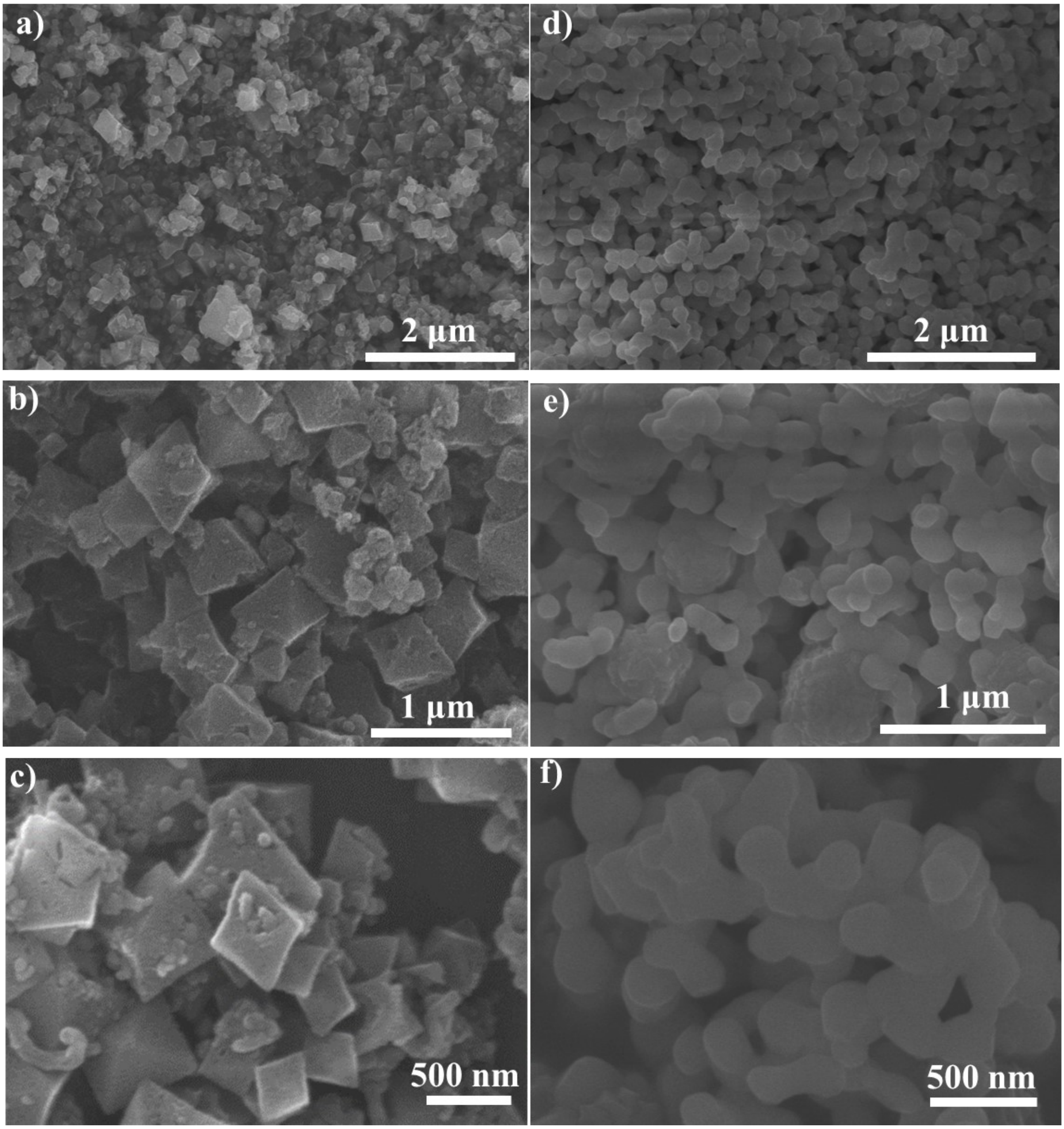


**Fig.S1.** SEM images of a-c) Fe-N/MC, d-f) Fe-N/C-ref at different scales.

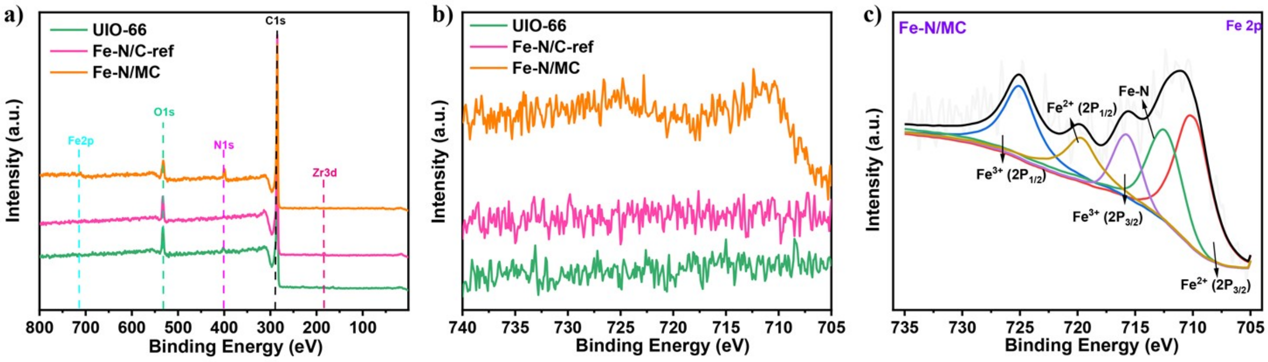


**Fig.S2** a) Survey XPS spectra, high-resolution; b) Fe2p XPS spectra of UIO, Fe-N/C-ref, Fe-N/MC; c) Fe2p XPS spectra of Fe-N/MC.

**Table S1.** Fraction of the different elements present in UIO, Fe-N/C-ref, and Fe-N/MC.

| **Sample** | **C %** | **N %** | **Fe %** |
|---|---|---|---|
| UIO-66 | 97.98 | 2.02 | / |
| Fe-N/C-ref | 97.77 | 1.91 | 0.32 |
| Fe/N/MC | 97.21 | 2.21 | 0.67 |

**Table S2.** Fraction of the different N species present in UIO, Fe-N/C-ref, and Fe-N/MC.

| Sample | Pyridinic N % | Fe-$N_X$ % | Pyrrolic-N % | Graphitic-N % | Oxidized-N % |
|---|---|---|---|---|---|
| UIO-66 | 10.41 | / | 37.23 | 14.28 | 38.48 |
| Fe-N/C-ref | 11.44 | 6.97 | 27.86 | 16.94 | 42.28 |
| Fe/N/MC | 26.06 | 9.51 | 16.25 | 23.33 | 27.88 |

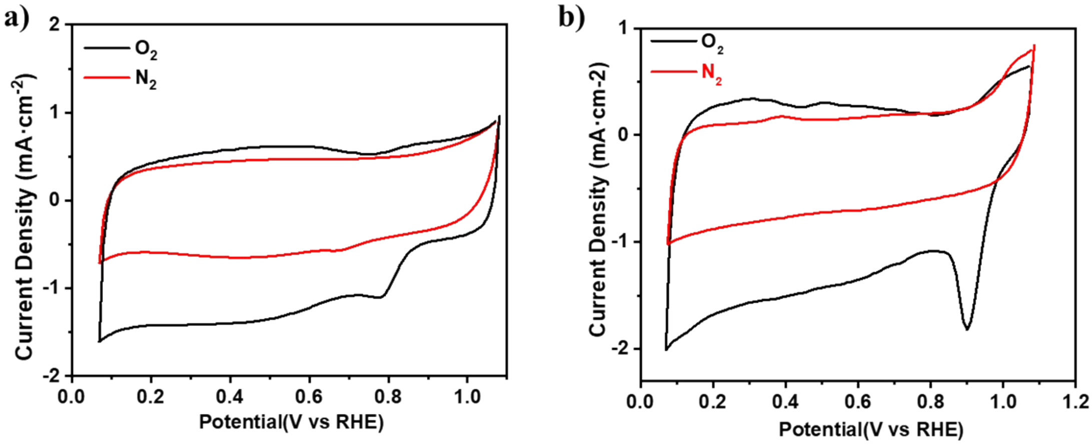


**Fig.S3** CV curves of Fe-N/MC in $N_2$ and $O_2$-saturated a) 0.1 M $HClO_4$ and b) 0.1 M KOH.

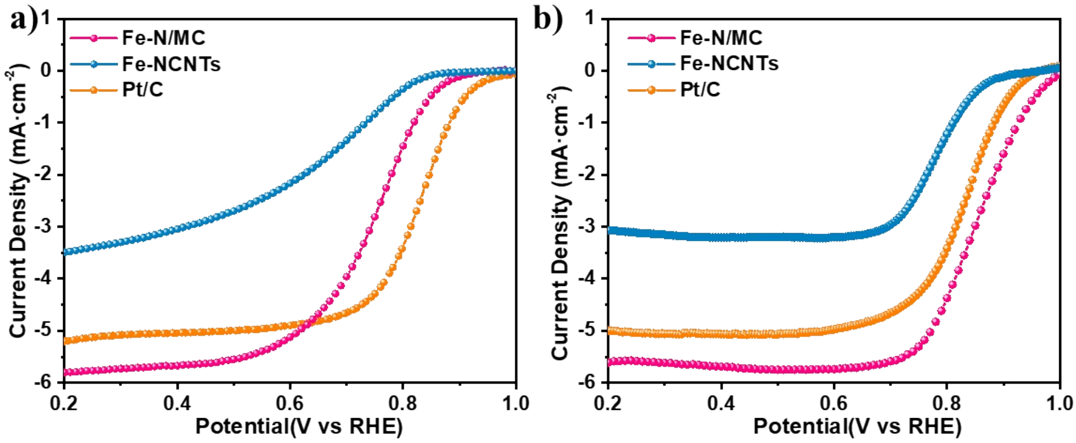


**Fig.S4** LSV ORR curves of Fe-NCNTs in $O_2$- saturated a) 0.1 M $HClO_4$ and b) 0.1 M KOH.

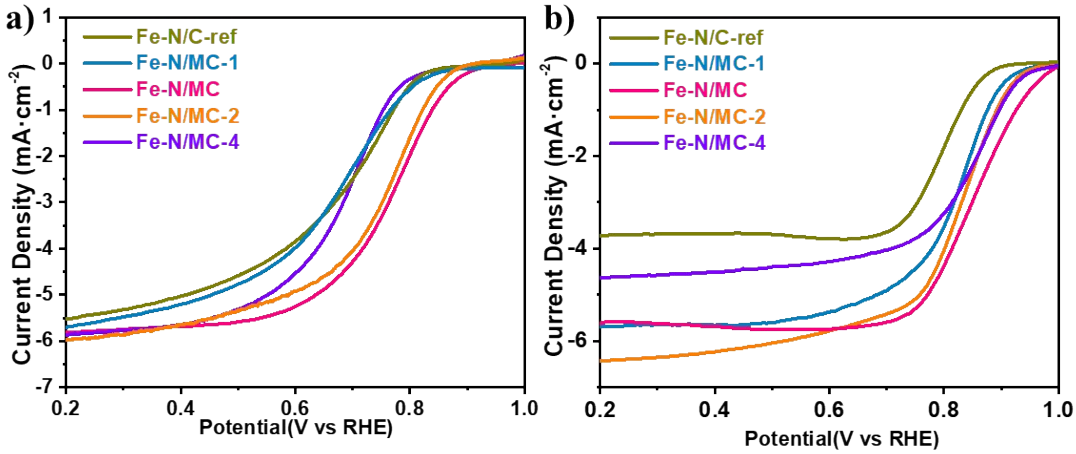


**Fig.S5** LSV ORR curves of Catalysts with FeCp with different doping levels in $O_2$- saturated a) 0.1 M $HClO_4$ and b) 0.1 M KOH.

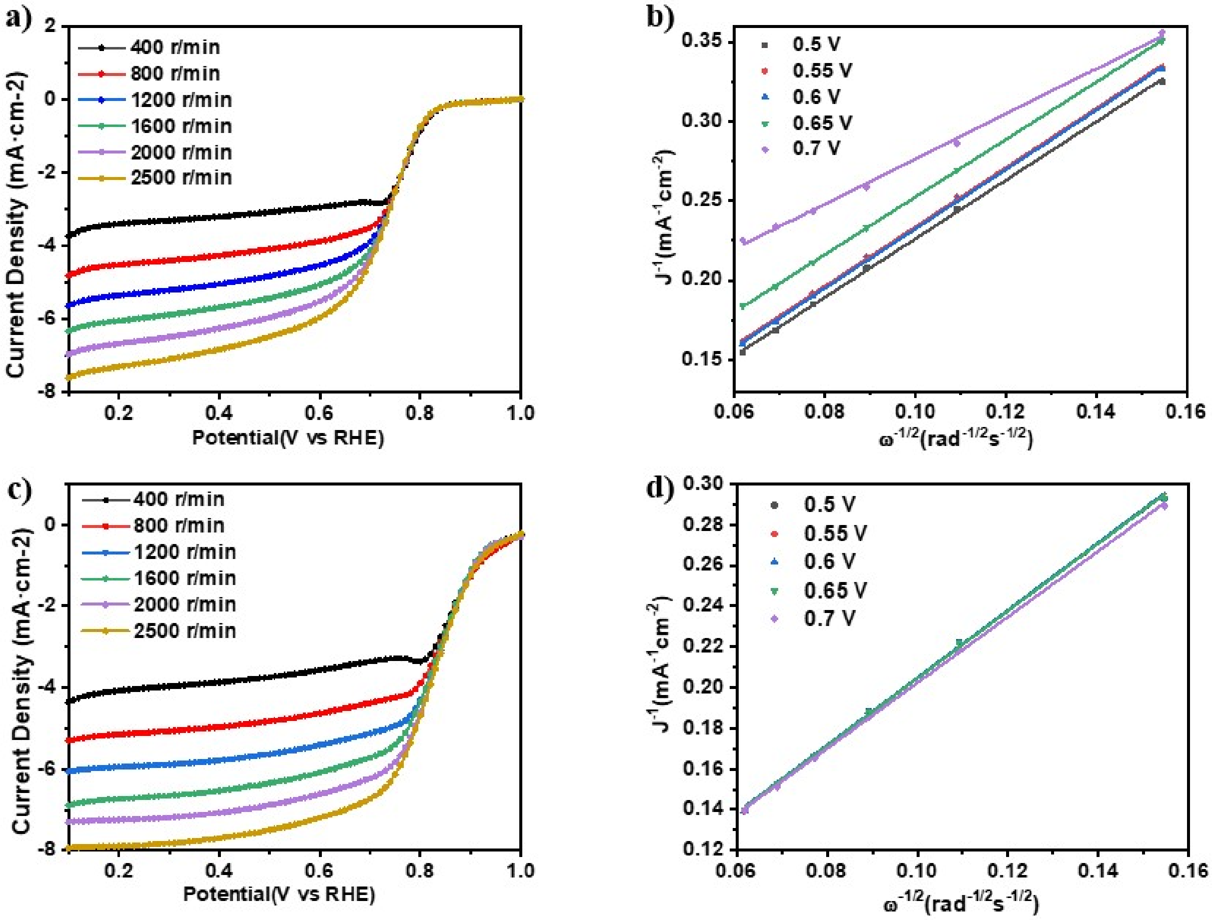


**Fig.S6** ORR curves of Fe-N/MC obtained at different rotation rates in $O_2$-saturated a) 0.1 M $HClO_4$ and c) KOH; K–L plots of $j^{-1}$ versus $\omega^{-1/2}$ on Fe-N/MC in $O_2$-saturated b) 0.1 M $HClO_4$ and d) KOH.

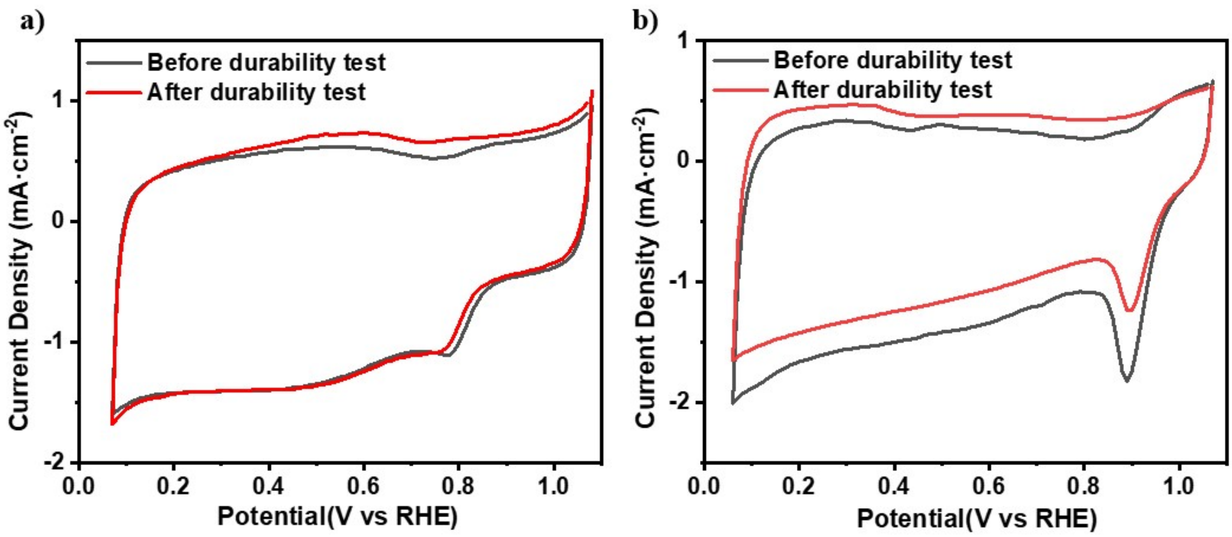


**Fig.S7** CV curves before and after durability test of Fe-N/MC in $O_2$-saturated a) 0.1 M $HClO_4$ and b) KOH**.**

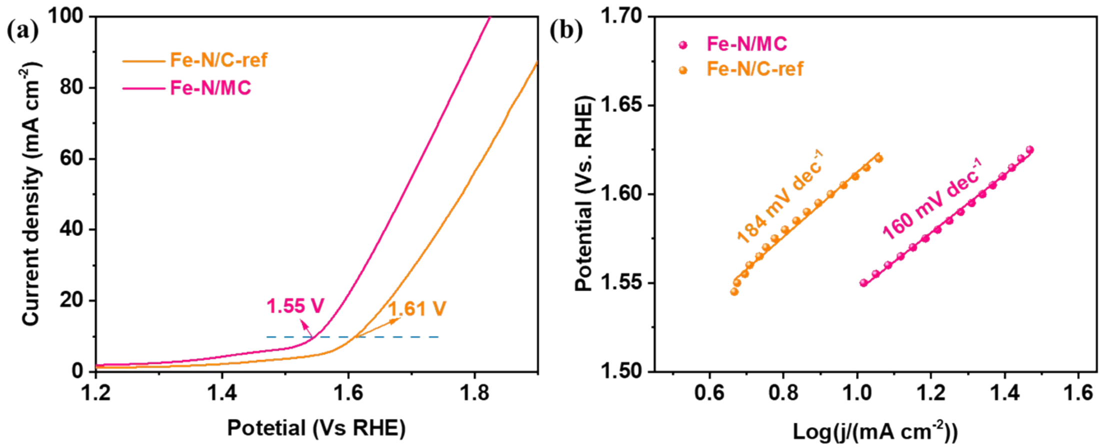


**Fig. S8** In 1 M KOH, (a) LSV curves for the OER of Fe-N/MC catalysts and Fe-N/C-ref catalysts at a scan rate of 10 mV s-1. (b) Tafel slope plot.

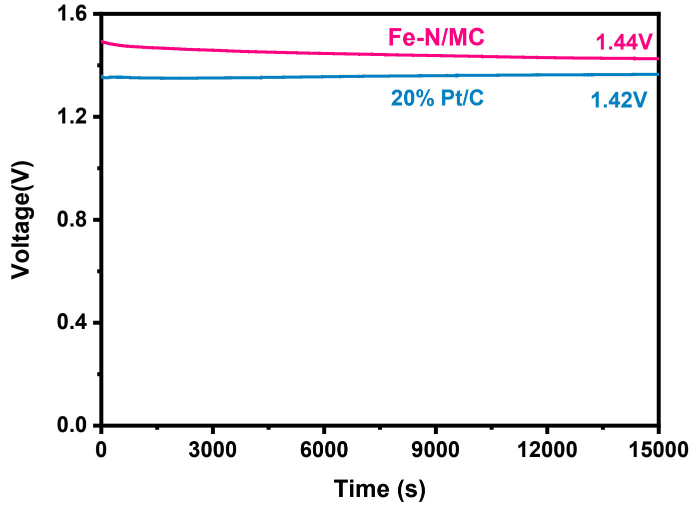


**Fig.S9** Open-circuit plots of Zn–air battery with Fe-N/MC and 20% Pt/C as the air cathode, respectively.

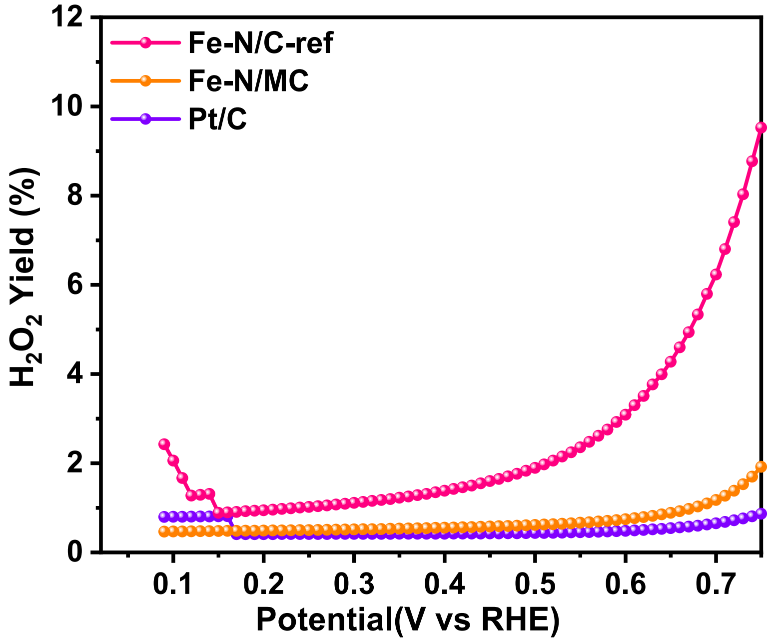


**Fig.S10** Hydrogen peroxide yields obtained from RRDE test results of Fe-N/C-ref, Fe-N/MC and Pt/C catalysts in oxygen-saturated 0.1 M $HClO_4$ solution.

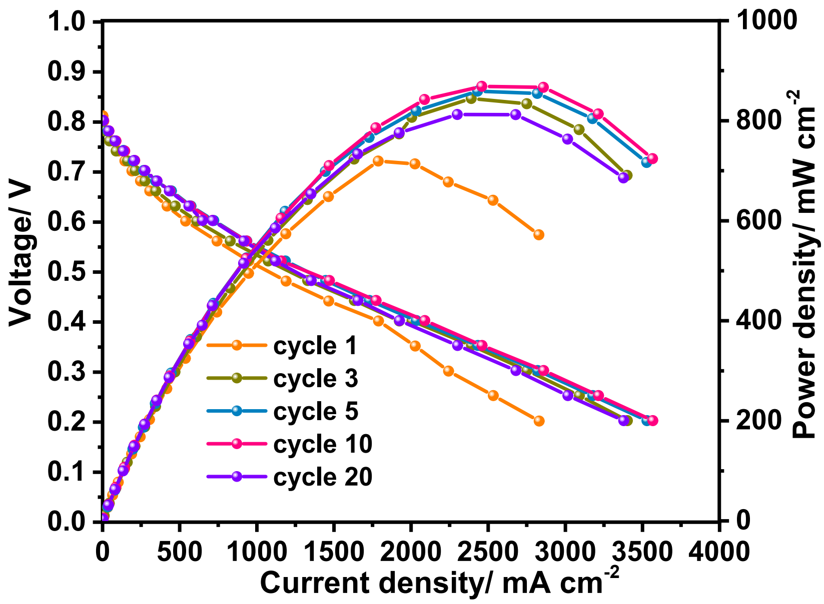


**Fig.S11.** IV curves of Fe-N/MC MEA after 24h discharging test

**Table S3.** Comparison of ORR performance of Fe-N/MC with other non-noble metal in alkaline medium

| Catalyst | $E_{onset}$vsRHE | $E_{1/2}$vsRHE | Catalyst loading ($mg/cm^2$) | References |
|---|---|---|---|---|
| **Fe-N/MC** | **0.95** | **0.85** | **0.5** | **This work** |
| Fe/N/S-PC | 0.97 | 0.87 | 0.5 | 1 |
| Fe/N/C(4mlm)-OAc | 0.95 | 0.844 | 0.6 | 2 |
| Fe-N/C-155 | 1.09 | 0.85 | 0.5 | 3 |
| FeN/C-800 | 0.923 | 0.809 | 0.1 | 4 |
| Co/N/C | 0.94 | 0.83 | 0.2 | 5 |
| $Fe_3C$@NG-800-0.2 | 0.98 | 0.83 | 0.5 | 6 |
| Fe/N/C | 0.94 | 0.83 | 0.5 | 7 |
| Fe-N/C | 1.019 | 0.848 | / | 8 |
| Fe3-NG | 0.965 | 0.826 | 0.5 | 9 |
| C-FeHZ8@g-$C_3N_4$-950 | 0.97 | 0.845 | 0.5 | 10 |

**Table S4.** Comparison of ORR performance of Fe-N/MC with other non-noble metal in acid medium

| Catalyst | $E_{onset}$vsRHE | $E_{1/2}$vsRHE | Catalyst loading ($mg/cm^2$) | References |
|---|---|---|---|---|
| **Fe-N/MC** | **0.88** | **0.76** | **0.5** | **This work** |
| PpPD-Fe-C | 0.826 | 0.718 | 0.9 | 11 |
| PCN-FeCo/C | 0.90 | 0.76 | 0.6 | 12 |
| C-FeZIF-900-0.84 | 0.90 | 0.77 | 0.5 | 13 |
| N, P-CGHNs | 0.90 | 0.68 | 0.6 | 14 |
| Fe-N-CNF | 0.84 | 0.62 | 0.6 | 15 |
| $FeN_4$/HOPC-c-1000 | / | 0.8 | 0.5 | 16 |
| $CeF_3$-Fe/N/C | 0.9 | 0.78 | 0.5 | 17 |
| Zn/Co(mlm)$_2$-P | 0.88 | 0.76 | 0.5 | 18 |
| Py-B12/C | / | 0.78 | 0.5 | 19 |
| $SiO_2$-Fe/N/C | / | 0.823 | 0.5 | 20 |

**Table S5.** Comparison of performance of the $H_2/O_2$ PEMFCs using the NPM cathode catalysts

| Catalyst | Operation temperature (℃) | Catalyst loading amount(mg cm$^{-2}$) | Maximum power density (mW cm$^{-2}$) | Back Pressure(bar) | References |
|---|---|---|---|---|---|
| **Fe-N/MC** | **70** | **4.0** | **1150** | **2** | **This work** |
| Fe/N/C-SCN | 80 | 4.0 | 1030 | 2 | 21 |
| CFeHZ8@g$C_3N_4$-950 | 80 | 1.0 | 775 | 2 | 10 |
| Co-N-C@F127 | 80 | 4 | 870 | 1 | 22 |
| (CM+PANI)-Fe-C | 80 | 4 | 940 | 2 | 23 |
| ZIF-FA-CNT-p | 80 | 4.5 | 820 | 2 | 24 |
| Fe/N/C(4mlm)-OAc | 80 | 3 | 1330 | 2 | 3 |
| $SiO_2$-Fe/N/C | 80 | 2.7 | 880 | 2 | 20 |
| Fe2-Z8-C | 80 | 2.8 | 1141 | 2 | 25 |
| Fe-MOF-100nm | 94 | 4 | 1140 | 1.7 | 26 |
| Fe/Phen/Z8 | 80 | 4 | 910 | 1 | 27 |

**Table S6.** The overall Fe content of Fe-N/MC and Fe-N/C-ref based on ICP-OES

| Sample | Total Fe (wt.%) | Fe (after acid treatment) (wt.%) |
|---|---|---|
| **Fe-N/MC** | 3.16 | 2.76 |
| **Fe-N/C-ref** | 2.07 | 1.48 |

**Table S7.** Comparison of the durability performance of PEMFCs using NPM cathode catalysts

| Catalyst | Test environment | Initial current density (mA $cm^{-2}$) | Performance degradation rate | times | References |
|---|---|---|---|---|---|
| **Fe-N/MC** | **$H_2$-$O_2$** | **651** | **42.3%** | **24h** | **This work** |
| Fe-ZIF'/CNT-1 | $H_2$-$O_2$ | 615 | 34% | 30h | 28 |
| Fe-N-C | H2-Air | 500 | 58% | 23h | 29 |
| $FeO_x$@GC-NOMC | $H_2$-$O_2$ | 440 | 28.9% | 150h | 30 |
| Fe/N/C-SCN | $H_2$-$O_2$ | 1600 | 71.9% | 100h | 21 |
| CFeHZ8@g$C_3N_4$ -950 | $H_2$-$O_2$ | 400 | 51.1% | 8h | 22 |
| ZIF-FA-CNT-p | $H_2$-$O_2$ | 1200 | 79.1% | 60h | 25 |
| Fe/N/C(4mlm)-OAc | $H_2$-$O_2$ | 2600 | 80.3% | 35h | 2 |
| CeF3-Fe/N/C | $H_2$-$O_2$ | 120 | 46% | 24h | 16 |
| SA-3DNC | $H_2$-$O_2$ | 380 | 25% | 20h | 31 |
| C-FeZIF-1.44-950 | $H_2$-$O_2$ | 1000 | 32.2% | 10h | 32 |

## References


[1] Zheng, L.; Dong, Y. Y.; Chi, B.; Cui, Z. M.; Deng, Y. J.; Shi, X. D.; Du, L.; Liao, S. J., UIO-66-NH2-Derived Mesoporous Carbon Catalyst Co-Doped with Fe/N/S as Highly Efficient Cathode Catalyst for PEMFCs. *Small* **2019,** *15* (4).

[2] Li, Y. Y.; Zhang, P. Y.; Wan, L. Y.; Zheng, Y. P.; Qu, X. M.; Zhang, H. K.; Wang, Y. S.; Zaghib, K.; Yuan, J. Y.; Sun, S. H.; Wang, Y. C.; Zhou, Z. Y.; Sun, S. G., A General Carboxylate-Assisted Approach to Boost the ORR Performance of ZIF-Derived Fe/N/C Catalysts for Proton Exchange Membrane Fuel Cells. *Adv Funct Mater* **2021,** *31* (15).

[3] Ye, G. Y.; He, Q.; Liu, S. Q.; Zhao, K. M.; Su, Y. K.; Zhu, W. W.; Huang, R. J.; He, Z., Cage-confinement of gas-phase ferrocene in zeolitic imidazolate frameworks to synthesize high-loading and atomically dispersed Fe-N codoped carbon for efficient oxygen reduction reaction. *J Mater Chem A* **2019,** *7* (27), 16508-16515.

[4] Lin, L.; Zhu, Q.; Xu, A. W., Noble-Metal-Free Fe-N/C Catalyst for Highly Efficient Oxygen Reduction Reaction under Both Alkaline and Acidic Conditions. *Journal of the American Chemical Society* **2014,** *136* (31), 11027-11033.

[5] Li, Z. H.; Shao, M. F.; Zhou, L.; Zhang, R. K.; Zhang, C.; Wei, M.; Evans, D. G.; Duan, X., Directed Growth of Metal-Organic Frameworks and Their Derived Carbon-Based Network for Efficient Electrocatalytic Oxygen Reduction. *Advanced Materials* **2016,** *28* (12), 2337-2344.

[6] Jiang, H. L.; Yao, Y. F.; Zhu, Y. H.; Liu, Y. Y.; Su, Y. H.; Yang, X. L.; Li, C. Z., Iron Carbide Nanoparticles Encapsulated in Mesoporous Fe-N-Doped Graphene-Like Carbon Hybrids as Efficient Bifunctional Oxygen Electrocatalysts. *Acs Appl Mater Inter* **2015,** *7* (38), 21511-21520.

[7] Ferrero, G. A.; Preuss, K.; Marinovic, A.; Jorge, A. B.; Mansor, N.; Brett, D. J. L.; Fuertes, A. B.; Sevilla, M.; Titirici, M. M., Fe-N-Doped Carbon Capsules with Outstanding Electrochemical Performance and Stability for the Oxygen Reduction Reaction in Both Acid and Alkaline Conditions. *Acs Nano* **2016,** *10* (6), 5922-5932.

[8] Zhang, W.; Xu, X.; Zhang, C.; Yu, Z.; Zhou, Y.; Tang, Y.; Wu, P.; Guo, S., 3D Space-Confined Pyrolysis of Double-Network Aerogels Containing In-Fe Cyanogel and Polyaniline: A New Approach to Hierarchically Porous Carbon with Exclusive Fe-N-x Active Sites for Oxygen Reduction Catalysis. *Small Methods* **2017,** *1* (8).

[9] Cui, X. Y.; Yang, S. B.; Yan, X. X.; Leng, J. G.; Shuang, S.; Ajayan, P. M.; Zhang, Z. J., Pyridinic-Nitrogen-Dominated Graphene Aerogels with Fe-N-C Coordination for Highly Efficient Oxygen Reduction Reaction. *Adv Funct Mater* **2016,** *26* (31), 5708-5717.

[10] Deng, Y. J.; Chi, B.; Tian, X. L.; Cui, Z. M.; Liu, E. S.; Jia, Q. Y.; Fan, W. J.; Wang, G. H.; Dang, D.; Li, M. S.; Zang, K. T.; Luo, J.; Hu, Y. F.; Liao, S. J.; Sun, X. L.; Mukerjee, S., g-C3N4 promoted MOF derived hollow carbon nanopolyhedra doped with high density/fraction of single Fe atoms as an ultra-high performance non-precious catalyst towards acidic ORR and PEM fuel cells. *J Mater Chem A* **2019,** *7* (9), 5020-5030.

[11] Zhu, Y. S.; Zhang, B. S.; Liu, X.; Wang, D. W.; Su, D. S., Unravelling the Structure of Electrocatalytically Active Fe-N Complexes in Carbon for the Oxygen Reduction Reaction. *Angew Chem Int Edit* **2014,** *53* (40), 10673-10677.

[12] Deng, Y. J.; Dong, Y. Y.; Wang, G. H.; Sun, K. L.; Shi, X. D.; Zheng, L.; Li, X. H.; Liao, S. J., Well-Defined ZIF-Derived Fe-N Codoped Carbon Nanoframes as Efficient Oxygen Reduction Catalysts. *Acs Appl Mater Inter* **2017,** *9* (11), 9699-9709.

[13] Yang, J.; Sun, H. Y.; Liang, H. Y.; Ji, H. X.; Song, L.; Gao, C.; Xu, H. X., A Highly Efficient Metal-Free Oxygen Reduction Electrocatalyst Assembled from Carbon Nanotubes and Graphene. *Advanced Materials* **2016,** *28* (23), 4606-4613.

[14] Wu, Z. Y.; Xu, X. X.; Hu, B. C.; Liang, H. W.; Lin, Y.; Chen, L. F.; Yu, S. H., Iron Carbide Nanoparticles

Encapsulated in Mesoporous Fe-N-Doped Carbon Nanofibers for Efficient Electrocatalysis. *Angew Chem Int Edit* **2015,** *54* (28), 8179-8183.

[15] Qiao, M.; Wang, Y.; Wang, Q.; Hu, G.; Mamat, X.; Zhang, S.; Wang, S., Hierarchically Ordered Porous Carbon with Atomically Dispersed FeN4 for Ultraefficient Oxygen Reduction Reaction in Proton-Exchange Membrane Fuel Cells. *Angew Chem Int Edit* **2020,** *59* (7), 2688-2694.

[16] Yin, X.; Utetiwabo, W.; Sun, S. H.; Lian, Y. M.; Chen, R. J.; Yang, W., Incorporation of CeF3 on single-atom dispersed Fe/N/C with oxophilic interface as highly durable electrocatalyst for proton exchange membrane fuel cell. *J Catal* **2019,** *374*, 43-50.

[17] Chong, L. N.; Goenaga, G. A.; Williams, K.; Barkholtz, H. M.; Grabstanowicz, L. R.; Brooksbank, J. A.; Papandrew, A. B.; Elzein, R.; Schlaf, R.; Zawodzinski, T. A.; Zou, J. X.; Ma, S. Q.; Liu, D. J., Investigation of Oxygen Reduction Activity of Catalysts Derived from Co and Co/Zn Methyl-Imidazolate Frameworks in Proton Exchange Membrane Fuel Cells. *Chemelectrochem* **2016,** *3* (10), 1541-1545.

[18] Chang, S. T.; Wang, C. H.; Du, H. Y.; Hsu, H. C.; Kang, C. M.; Chen, C. C.; Wu, J. C. S.; Yen, S. C.; Huang, W. F.; Chen, L. C.; Lin, M. C.; Chen, K. H., Vitalizing fuel cells with vitamins: pyrolyzed vitamin B12 as a non-precious catalyst for enhanced oxygen reduction reaction of polymer electrolyte fuel cells. *Energ Environ Sci* **2012,** *5* (1), 5305-5314.

[19] Li, J.; Chen, M.; Cullen, D. A.; Hwang, S.; Wang, M.; Li, B.; Liu, K.; Karakalos, S.; Lucero, M.; Zhang, H.; Lei, C.; Xu, H.; Sterbinsky, G. E.; Feng, Z.; Su, D.; More, K. L.; Wang, G.; Wang, Z.; Wu, G., Atomically dispersed manganese catalysts for oxygen reduction in proton-exchange membrane fuel cells. *Nature Catalysis* **2018,** *1* (12), 935-945.

[20] Yang, X. H.; Wang, Y. C.; Zhang, G. X.; Du, L.; Yang, L. J.; Markiewicz, M.; Choi, J. Y.; Chenitz, R.; Sun, S. H., SiO2-Fe/N/C catalyst with enhanced mass transport in PEM fuel cells. *Appl Catal B-Environ* **2020,** *264*.

[21] Y.C. Wang, Y.J. Lai, L. Song, Z.Y. Zhou, J.G. Liu, Q. Wang, X.D. Yang, C. Chen, W. Shi, Y.P. Zheng, M. Rauf, S.G. Sun, S-Doping of an Fe/N/C ORR Catalyst for Polymer Electrolyte Membrane Fuel Cells with High Power Density, Angew Chem Int Edit, 54 (2015) 9907-9910

[22] He, Y.; Hwang, S.; Cullen, D. A.; Uddin, M. A.; Langhorst, L.; Li, B.; Karakalos, S.; Kropf, A. J.; Wegener, E. C.; Sokolowski, J.; Chen, M.; Myers, D.; Su, D.; More, K. L.; Wang, G.; Litster, S.; Wu, G., Highly active atomically dispersed CoN4 fuel cell cathode catalysts derived from surfactant-assisted MOFs: carbon-shell confinement strategy. *Energ Environ Sci* **2019,** *12* (1), 250-260.

[23] Strickland, K.; Miner, E.; Jia, Q.; Tylus, U.; Ramaswamy, N.; Liang, W.; Sougrati, M.-T.; Jaouen, F.; Mukerjee, S., Highly active oxygen reduction non-platinum group metal electrocatalyst without direct metal-nitrogen coordination. *Nature Communications* **2015,** *6*.

[24] Zhang, C.; Wang, Y. C.; An, B.; Huang, R. Y.; Wang, C.; Zhou, Z. Y.; Lin, W. B., Networking Pyrolyzed Zeolitic Imidazolate Frameworks by Carbon Nanotubes Improves Conductivity and Enhances Oxygen-Reduction Performance in Polymer-Electrolyte-Membrane Fuel Cells. *Advanced Materials* **2017,** *29* (4).

[25] Liu, Q.; Liu, X.; Zheng, L.; Shui, J., The Solid-Phase Synthesis of an Fe-N-C Electrocatalyst for High-Power Proton-Exchange Membrane Fuel Cells. *Angew Chem Int Edit* **2018,** *57* (5), 1204-1208.

[26] Uddin, A.; Dunsmore, L.; Zhang, H. G.; Hu, L. M.; Wu, G.; Litster, S., High Power Density Platinum Group Metal-free Cathodes for Polymer Electrolyte Fuel Cells. *Acs Appl Mater Inter* **2020,** *12* (2), 2216-2224.

[27] Fu, X. G.; Zamani, P.; Choi, J. Y.; Hassan, F. M.; Jiang, G. P.; Higgins, D. C.; Zhang, Y. N.; Hoque, M. A.; Chen, Z. W., In Situ Polymer Graphenization Ingrained with Nanoporosity in a Nitrogenous Electrocatalyst Boosting the Performance of Polymer-Electrolyte-Membrane Fuel Cells. *Advanced Materials* **2017,** *29* (7).

[28] Xia, D. S.; Tang, F.; Yao, X. Z.; Wei, Y. P.; Cui, Y. F.; Dou, M.; Gan, L.; Kang, F. Y., Seeded growth

of branched iron-nitrogen-doped carbon nanotubes as a high performance and durable non-precious fuel cell cathode. *Carbon* **2020,** *162*, 300-307.

[29] F. Xiao, G.L. Xu, C.J. Sun, I. Hwang, M.J. Xu, H.W. Wu, Z.D. Wei, X.Q. Pan, K. Amine, M.H. Shao, Durable hybrid electrocatalysts for proton exchange membrane fuel cells, Nano Energy, **2020**, 77.

[30] K. Wang, H.X. Chen, X.F. Zhang, Y.X. Tong, S.Q. Song, P. Tsiakaras, Y. Wang, Iron oxide@graphitic carbon core-shell nanoparticles embedded in ordered mesoporous N-doped carbon matrix as an efficient cathode catalyst for PEMFC, Appl Catal B-Environ, **2020,** *264*.

[31] Y.H. Qian, Q.T. Liu, E. Sarnello, C.H. Tang, M.L. Chng, J.L. Shui, T. Li, S.J. Pennycook, M. Han, D. Zhao, MOF-Derived Carbon Networks with Atomically Dispersed Fe-N-x Sites for Oxygen Reduction Reaction Catalysis in Acidic Media, Acs Mater Lett, **2019,** *1* (1), 37-43.

[32] Y. Deng, B. Chi, J. Li, G. Wang, L. Zheng, X. Shi, Z. Cui, L. Du, S. Liao, K. Zang, J. Luo, Y. Hu, X. Sun, Atomic Fe-Doped MOF-Derived Carbon Polyhedrons with High Active-Center Density and Ultra-High Performance toward PEM Fuel Cells, Adv Energy Mater, **2019,** *9* (13).